tal help of S. Brennan, M. Hecht, and J. N. Miller. We would like to thank I. Lindau and W. E. Spicer for providing the data acquisition system.

This work was partly supported by the National Science Foundation under Contract No. DMR 77-27489 in cooperation with SLAC and the Basic Energy Division of the Department of Energy.

[1]S. A. Flodström, C. W. B. Martinson, R. Z. Bachrach, S. B. M. Hagström, and R. S. Bauer, Phys. Rev. Lett. 40, 907 (1978).

[2]W. Eberhardt and F. J. Himpsel, Phys. Rev. Lett. 42, 1375 (1979); C. W. B. Martinson and S. A. Flodström, Solid State Commun. 30, 671 (1979).

[3]R. Payling and J. A. Ramsay, in Proceedings of the Fifth Australian Vacuum Conference, Brisbane, 1976 (unpublished), p. 131.

[4]C. W. B. Martinsson, S. A. Flodström, J. Rundgren, and P. Westrin, to be published.

[5]D. R. Salahub, M. Roche, and R. P. Messmer, Phys. Rev. B 18, 6495 (1978).

[6]P. O. Gartland, Surf. Sci. 62, 183 (1977).

[7]P. Hofmann, W. Wyrobisch, and A. M. Bradshaw, Surf. Sci. 80, 344 (1979).

[8]N. D. Lang and A. R. Williams, Phys. Rev. Lett. 34, 531 (1975).

[9]K. Y. Yu, J. N. Miller, P. Chye, W. E. Spicer, N. D. Lang, and A. R. Williams, Phys. Rev. B 14, 1446 (1976).

[10]D. E. Sayers, F. W. Lytle, and E. A. Stern, Phys. Rev. Lett. 27, 1204 (1971).

[11]P. H. Citrin, P. Eisenberger, and R. C. Hewitt, Phys. Rev. Lett. 41, 309 (1978).

[12]J. Stöhr, D. Denley, and P. Perfetti, Phys. Rev. B 18, 4132 (1978).

[13]E. A. Stern, D. E. Sayers, J. G. Dash, H. Shechter, and B. Bunker, Phys. Rev. Lett. 38, 767 (1977); G. S. Brown, P. Eisenberger, and P. Schmidt, Solid State Commun. 24, 201 (1977).

[14]F. C. Brown, R. Z. Bachrach, and N. Lien, Nucl. Instrum. Methods 152, 73 (1978). For the present experiments a holographic 1200-line/mm grating was installed as discussed by J. Stöhr and L. I. Johansson, to be published.

[15]J. Stöhr, L. I. Johansson, I. Lindau, and P. Pianetta, Phys. Rev. B 20, 664 (1979).

[16]J. Stöhr, L. I. Johansson, S. Brennan, M. Hecht, and J. N. Miller, to be published.

[17]P. A. Lee, Boon-Keng Teo, and A. L. Simmons, J. Am. Chem. Soc. 99, 3856 (1977); Boon-Keng Teo and P. A. Lee, to be published.

[18]J. C. Slater, *Symmetry and Energy Bands in Crystals* (Dover, New York, 1972), pp. 308–346.

Evidence for Possible Electronic Contributions to the W(001) Surface Phase Transition

H. Krakauer, M. Posternak, and A. J. Freeman

Department of Physics, Northwestern University, Evanston, Illinois 60201

(Received 10 September 1979)

The calculated surface generalized susceptibility, determined from *ab initio* self-consistent thin-film energy bands for the unreconstructed phase of W(001), displays a prominent peak at $\bar{M}$ when matrix elements and local-field corrections are included and supports proposed charge-density-wave interpretations of the observed reconstruction to the $c(2\times2)$ phase. These results are consistent with the Debe and King parallel-shift model and the suggestion that W(001)$c(2\times2)$-H at room temperature represents an impurity-stabilized substrate reconstruction.

Surface-structural phase transitions are becoming a subject of intense experimental and theoretical investigation. A prototypical example is given in the low-energy-electron-diffraction (LEED) studies of the tungsten[1,2] (001) surface which show a temperature-dependent phase transition to a $(\sqrt{2}\times\sqrt{2})R45°$ or $c(2\times2)$ structure when the temperature is lowered below about 300 K. This transformation seems to be of second order and is reversible on varying only the temperature. [A similar transition has been observed on Mo(001).[2]] Recent investigations[1,2] conclude that chemisorbed impurities (hydrogen in particular) need not be present on the surface when the $c(2\times2)$ structure is observed, thus implying that the transition is characteristic of the clean surface.

Felter, Barker, and Estrup[1] and Debe and King[2] have suggested that relatively small periodic distortions could account for the phase transition, and they have noted that this is compatible with a charge-density-wave (CDW) mechanism as in the layered transition-metal dichalcogenides. A LEED intensity analysis[3] for W(001) at 100–140 K supports a model proposed by Debe and King[4] in-

volving atomic shifts parallel to the plane of the surface with the shifts in the ⟨110⟩ direction. The shifts were found to be in the range 0.15–0.3 Å.[3] This model is consistent with the observed lack of fourfold symmetry in the LEED pattern.[4] Recently, however, Tsong and Sweeney[5] presented fully resolved atomic images of the W(001) plane obtained with a field-ion microscope at 21 K showing no loss of fourfold symmetry. Thus, the precise nature of the low-temperature phase has not been unquestionably determined.

The CDW mechanism has been proposed for the reconstruction of semiconductor surfaces by Tosatti and Anderson,[6] and Tosatti[7] has suggested that in W(001) and Mo(001) a surface-resonance (SR) band near E_F might drive the transition via surface-phonon softening and gapping of the two-dimensional Fermi surface (2D FS) accompanying the onset of a CDW. Using Green's functions obtained in a non-self-consistent surface calculation, Inglesfield[8] has calculated the surface electronic response for Mo(001). His results, however, show only an extremely small Kohn anomaly due to the Sr states, and he concludes, in contradiction to earlier suggestions,[1,2,7] that the transition is not due to the temperature dependence of the Fermi distribution as in CDW systems.

This Letter presents results of calculations of the generalized susceptibility, $\chi(\vec{q})$, including matrix elements and local-field effects for W(001) using our self-consistent semirelativistic electronic energies and wave functions obtained for a seven-layer film.[9] We find a prominent peak at the zone boundary $\bar{M}$ when local-field corrections are included. These results provide theoretical evidence indicating that the phase transition may indeed be electronically driven in agreement with the CDW mechanism. Our results are shown to be consistent not only with the parallel shift model on clean W(001),[3,4] but also with results concerning W(001)$c(2\times2)$-H at room temperature where Barker and Estrup[10] have suggested that the superstructure involves displacements of W atoms (reconstruction of the substrate) and that the role of hydrogen is one of impurity stabilizer.

As details of the film calculation are presented elsewhere,[9] we only briefly describe some of the pertinent results obtained with our recently developed self-consistent linearized-augmented-plane-wave (LAPW) method for thin films including all relativistic effects except spin-orbit. Figure 1 shows those surface states (SS) and SR states having a localization greater than 70% in the two outermost layers. These results are in good agreement with detailed angularly resolved photoemission-spectroscopy measurements[11] with respect to both the energy and symmetry of the SS and SR states. Self-consistency is crucial in obtaining reliable results for the SS on W(001) (Ref. 9) and Mo(001) (Ref. 12): Most non-self-consistent calculations have not found the very localized SS at $\bar{\Gamma}$ just below the Fermi energy (Fig. 1), although this state is very prominent in photoemission measurements.[11]

The electronic response to a perturbation with wave vector $\vec{q}$ is determined by the generalized susceptibility matrix $\underline{\chi}_{sc}=\underline{\chi}\underline{\epsilon}^{-1}$, where the dielectric matrix, $\underline{\epsilon}$, can be expressed in terms of the bare susceptibility, $\underline{\chi}$, as $\underline{\epsilon}=\underline{1}-\underline{V}\underline{\chi}$, and $\underline{V}$ is the Fourier transform of the electron-electron interaction. The determination of χ is of great interest because of its possible role in revealing instabilities in the electronic ground state, e.g., spin-density waves and CDW,[13] through the resonancelike increase of ϵ^{-1}. The expression for χ is given by

$$\chi_{\text{layer}}(\vec{q}+\vec{G},\vec{q}+\vec{G}')=\sum_{\substack{\vec{k},\vec{k}'\\ n,n'}}\frac{f_{\vec{k}}^{n}(1-f_{\vec{k}'}^{n'})}{E_{\vec{k}}^{n}-E_{\vec{k}'}^{n'}}M_{kk'}^{nn'}(\vec{q}+\vec{G})M_{kk'}^{nn'*}(\vec{q}+\vec{G}'). \tag{1}$$

Here $M_{kk'}^{nn'}=\langle\Psi_k^n|e^{-i(\vec{q}+\vec{G})\vec{r}}|\Psi_{k'}^{n'}\rangle_{\text{layer}}$, $\vec{q}=(q_x,q_y,0)$, $\vec{k}$ is the 2D Bloch momentum, $E_{\vec{k}}^{n}$ is the energy of the 2D Bloch wave function Ψ_k^n with band index n and occupation number $f_{\vec{k}}^{n}$, and $\vec{G}$ and $\vec{G}'$ are 2D reciprocal-lattice vectors. The matrix element M imposes the restriction $\vec{k}'=\vec{k}+\vec{q}+\vec{K}$, where $\vec{K}$ is a 2D reciprocal-lattice vector which reduces $\vec{k}'-\vec{k}$ to the first 2D Brillouin zone, and the volume of integration can be one or more layers. The 2D Brillouin-zone integrations for χ in Eq. (1) were performed with a 2D adaptation of the analytic tetrahedron method.[14] Energies and wave functions were calculated at fifteen $\vec{k}$ points in the $\frac{1}{8}$ irreducible BZ, which is divided into sixteen microtriangles in which the 2D $\vec{k}$-space integration is performed analytically. Inside a given microtriangle, the $\vec{k}$ dependence of $M_{kk'}$ is neglected and $M_{kk'}$ is evaluated at the center of the microtriangle. The full LAPW wave function Ψ_k

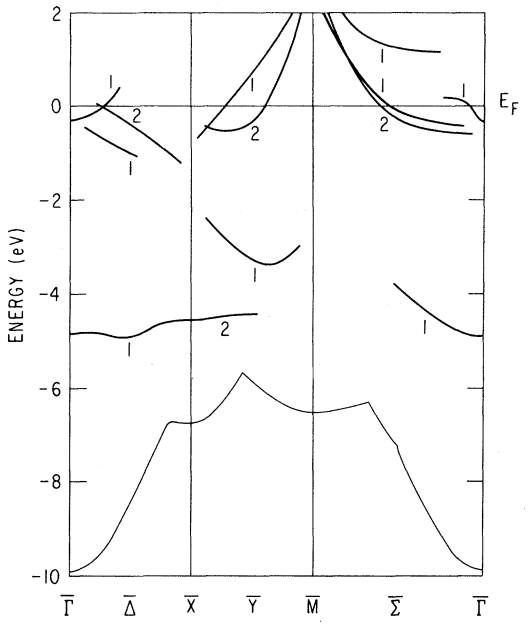

FIG. 1. Surface states and surface resonance states for the seven-layer W(001) film. The bottom of the conduction band is outlined along the lower part of the figures.

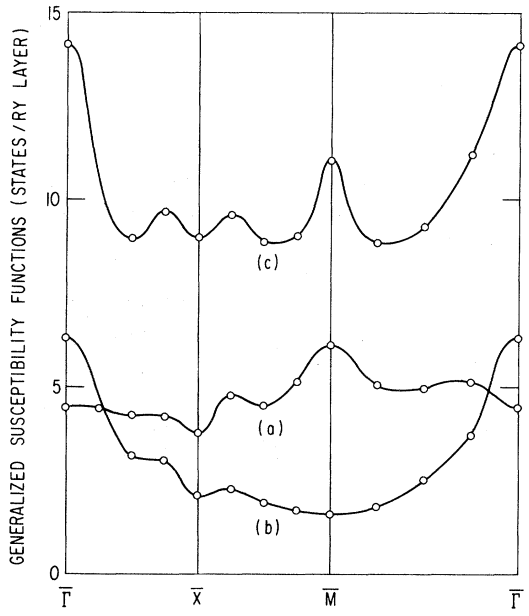

FIG. 2. Susceptibility functions for the surface layer. Curves *a*, *b*, and *c* are described in the text.

is approximated by extending the interstitial plane-wave representation into the muffin-tin spheres and into part of the vacuum region and renormalizing Ψ_k. This can be justified by the fact that each LAPW basis function matches with continuous derivative across the various boundaries, so that sensible behavior can be expected in a large region of the muffin-tin spheres and vacuum while strictly preserving symmetry selection rules. The localization in each layer of the wave function is typically within 5–10% of the correct value, and different states with identical symmetry are orthogonal to the same accuracy: $\langle \Psi_{k'}{}^{n'} | \times | \Psi_k{}^n \rangle_{\text{all space}} \leq 0.05$–$0.10$ unless $(n',k') = (n,k)$. States of different symmetry are exactly orthogonal.

The calculated results for χ in the surface layer are shown in Fig. 2. All states within 2 eV above and below the Fermi energy, E_F, were included. Curve *a* corresponds roughly to the constant-matrix-element approximation for the intraband ($n = n'$) part of $\chi(\vec{q})$ with $\vec{G} = \vec{G}' = 0$, where we have replaced $M_{kk'}{}^{nn} M_{kk'}{}^{nn*}$ by $W_k{}^n W_{k'}{}^n$, and $W_k{}^n = \langle \Psi_k{}^n | \Psi_k{}^n \rangle_{\text{layer}}$ is the weight or localization of the state in the given layer of the film. Here, $W_k{}^n$ is determined from the exact wave function, and this approximation yields the correct result for the intraband part at $\vec{q} = 0$. There is a definite peak at $\bar{M}$ [$\vec{q} = (1,1)\pi/a$] which is due to 2D, Fermi-surface nesting of the SR states midway between $\bar{\Gamma}$ and $\bar{M}$ in Fig. 1 (shifting E_F by $\sim \pm 0.14$ eV reduces the peak at $\bar{M}$ by about 30%). $\chi(\vec{q} = 0)$ in this case is related to the layer-projected density of states for the surface layer. The interband part of $\chi(\vec{q})$ in this approximation (not shown) has relatively little structure and is about 10 times as large. $\chi(\vec{q})$ for the other layers is comparatively featureless and smaller by about a factor of 3, reflecting the sizable contribution of the localized SS and SR states in the surface layer. The effect of including the matrix elements (extending the plane-wave representation for $\Psi_k{}^n$ as discussed above) is shown in curve *b* which pictures tht total (intraband plus interband) $\chi(\vec{q})$. The most dramatic effect of including matrix elements is to remove completely the peak at the nesting vector $\bar{M}$ in curve *a*. The difference in value of curves *a* and *b* at $\bar{\Gamma}$ is due to the fact that *b* includes a small interband contribution (this is nonzero because the volume of integration in $M_{kk'}{}^{nn'}$ is only over a single layer). The intraband part of *b* at $\bar{\Gamma}$ differs from *a* by 10%, since the intraband matrix elements, $M_{kk'}{}^{nn'}$, in *b* reduce to the layer weights derived from the plane-wave representation of $\Psi_k{}^n$. Local-field corrections, so far neglected, can be large,[15] however, in transition metals where the off-diagonal elements $\chi(\vec{q}+\vec{G}, \vec{q}+\vec{G}')$ are not insignificant compared to $\chi(\vec{q})$. Following

Gupta and Sinha[16] these corrections can be estimated by making the *Ansatz* $\chi(\vec{q}+\vec{G},\vec{q}+\vec{G}')=A(\vec{q}+\vec{G})\hat{\chi}(\vec{q})A(\vec{q}+\vec{G}')$, where $\hat{\chi}(\vec{q})$ is $\chi(\vec{q})$ with matrix elements set equal to 1 and $A(\vec{q}+\vec{G})$ is an averaged matrix element $M_{kk'}(\vec{q}+\vec{G})$ over all allowed transitions. Neglecting the $\vec{q}$ dependence of the electron-electron interaction V then yields the following results for the screened susceptibility: $\chi_{sc}(\vec{q},\vec{q})=\chi(\vec{q})/[1-VF(\vec{q})]$, where $F(\vec{q})=\sum_{\vec{G}}\chi(\vec{q}+\vec{G},\vec{q}+\vec{G})$. Thus local-field corrections, in this approximate treatment, result in $F(\vec{q})$ entering the denominator in place of the usual $\chi(\vec{q})$. The results for $F(\vec{q})$ are shown in curve c, which reveals a prominent peak restored at the nesting vector $\bar{M}$. Curve c was obtained by retaining all $\vec{G}$ vectors satisfying $|\vec{q}+\vec{G}|^2\leq 10(\pi/a)^2$ in the summation for $F(\vec{q})$. We have investigated the convergence of $F(\vec{q})$ with respect to $\vec{G}$ vectors by calculating $F(\vec{q})$ at $\bar{\Gamma},\bar{X}$, and $\bar{M}$ for two larger sets of $\vec{G}$ vectors: $|\vec{q}+\vec{G}|^2\leq 18(\pi/a)^2$ and $26(\pi/a)^2$. The overall magnitude of $F(\vec{q})$ at these points increases by an additional 10–20% for $|\vec{q}+\vec{G}|<18(\pi/a)^2$, and by another 6–10% for $|\vec{q}+\vec{G}|<26(\pi/a)^2$. In addition, the relative magnitudes remain the same to within about 10%.

The overall behavior in going from curve a to b to c in Fig. 2 is similar to that found previously for bulk Cr (Ref. 16) and Sc.[17] In these cases, absolute peaks were found at physically significant nesting vectors when the constant-matrix-element approximation was used for χ. In both cases, though, including matrix elements completely removed the peak at the nesting vector, but an absolute peak was restored when local-field corrections were also incorporated. Note, however, that at the level of approximation used in curve c [(i) approximate matrix elements, (ii) simplified treatment of the local-field corrections, and (iii) truncation of the $\vec{G}$ summation in $F(\vec{q})$] the value of $F(\vec{q}=0)$ is about 25% larger than at $\bar{M}$. Nevertheless, an absolute maximum in $F(\vec{q})$ at $\vec{q}=0$ cannot lead to a soft-mode instability, since $\lim_{q\to 0}\epsilon(\vec{q},\vec{q})=(1+\text{const}/q^2)$ is the correct limit for a metal, and, therefore, ϵ^{-1} (which enters into the phonon dynamical matrix) is regular as $\vec{q}\to 0$.

When a structural phase transformation proceeds via a "soft-mode" instability, it is possible to represent the static distortions characterizing the structural rearrangements by a set of "frozen-in" phononlike displacements. Tosatti[7] has noted that the parallel-shift model[4] exactly fits an $\bar{M}_5$-(11) polarized phonon. This is precisely the vector for which our detertimation of χ shows a relative maximum (at $\bar{M}$ in Fig. 2). The conduction-electron response function of the unreconstructed W(001) surface thus reveals a possible instability at the zone boundary $\bar{M}$, and this supports the CDW interpretation for the phase transition in which the onset of the 2D CDW must be screened by an overdamping of the corresponding phonon mode, leading to the parallel-shift model. An instability with respect to CDW formation might also explain why hydrogen could act as an impurity stabilizer in the formation of W(001)$c(2\times 2)$-H at room temperature. As noted above, it has been suggested[10] that the superstructure involves reconstruction of the W substrate. This could occur if the interaction between the H atoms and the CDW stabilizes the excitonic ground state at higher temperatures by the addition of a "pinning" term in the Landau free energy. An impurity on the surface presumably has greater freedom to hop to different sites than does an impurity in a bulk solid. It may then be possible for the H atoms to settle at favorable sites and thus stabilize the commensurable CDW.

We are grateful to D. D. Koelling for close collaboration on the LAPW W(001) thin-film calculation,[9] and to W. Pickett for numerous helpful discussions of this work. This work was supported in part by the U. S. National Science Foundation under Grant No. 77-23776, in part by the U. S. Air Force Office of Scientific Research, and in part by the Swiss National Science Foundation and the American-Swiss Foundation for Scientific Exchange.

[1]T. E. Felter, R. A. Barker, and P. J. Estrup, Phys. Rev. Lett. 38, 1138 (1977).

[2]M. K. Debe and D. A. King, J. Phys. C 10, L303 (1977).

[3]R. A. Barker, P. J. Estrup, F. Jona, and P. M. Marcus, Solid State Commun. 25, 375 (1978).

[4]M. K. Debe and D. A. King, Phys. Rev. Lett. 39, 708 (1977).

[5]T. T. Tsong and J. Sweeney, Solid State Commun. 30, 767 (1979).

[6]E. Tosatti and P. W. Anderson, Solid State Commun. 14, 773 (1974).

[7]E. Tosatti, Solid State Commun. 25, 637 (1978).

[8]J. E. Inglesfield, J. Phys. C 12, 149 (1979).

[9]M. Posternak, H. Krakauer, A. J. Freeman, and D. D. Koelling, to be published; H. Krakauer, M. Posternak, and A. J. Freeman, Phys. Rev. B 19, 1706 (1979).

[10]R. A. Barker and P. J. Estrup, Phys. Rev. Lett. 41, 1307 (1978).

[11]S.-L. Weng, E. W. Plummer, and T. Gustafsson,

Phys. Rev. B 18, 1718 (1978).
[12]G. P. Kerker, Y. M. Ho, and M. L. Cohen, Phys. Rev. Lett. 40, 1593 (1978).
[13]S. K. Chan and V. Heine, J. Phys. F 3, 795 (1973).
[14]J. Rath and A. J. Freeman, Phys. Rev. B 11, 2109 (1975).
[15]S. K. Sinha, R. P. Gupta, and D. L. Price, Phys. Rev. B 9, 2564, 2573 (1974).
[16]R. P. Gupta and S. K. Sinha, Phys. Rev. B 3, 2401 (1971).
[17]R. P. Gupta and A. J. Freeman, Phys. Rev. B 13, 4376 (1976).

Superconductivity and the Metal-Nonmetal Transition in Hg-Xe Films

K. Epstein, E. D. Dahlberg, and A. M. Goldman
School of Physics and Astronomy, University of Minnesota, Minneapolis, Minnesota 55455
(Received 5 September 1979)

The electrical conductivities and transition temperatures of films consisting of random mixtures of Hg and Xe condensed onto substrates held at 4.2 K have been measured. A metal-nonmetal transition in which the temperature coefficient of resistance changes from positive to negative has been found near a volume fraction close to that expected for random percolation. This transition is accompanied by a substantial drop in the superconducting transition temperature which is measured resistively.

The electrical properties of alloys of metals and rare gases prepared by condensation onto cold substrates have been a subject of considerable experimental and theoretical interest.[1] In this Letter we report the results of an investigation into the properties of the Hg-Xe system, which has been extended beyond the work of others[2-4] to low enough temperatures so as to permit the observation of the effects of dilution of the Hg atoms by Xe on the superconductivity of the resultant films. The results of the present investigation are also different from those reported for the superconductivity of the Al-SiO_2 system which also exhibits a metal-nonmetal transition but which is granular.[5] Here we discuss the systematics of the variation of film resistance with Xe concentration and the composition dependence of the superconducting transition temperature.

Hg-Xe films would be expected to be model systems for the study of the effects of local order on conductivity and superconductivity provided that the films were indeed random and noncrystalline mixtures of their constituents. A way which should ensure this is to evaporate the films onto substrates kept at low temperatures and at the same time minimize the heating of surfaces by thermal radiation from the vapor source and by the kinetic energy of the atoms in vapor.[6] Both of these goals can be achieved with molecular-beam deposition techniques. The present apparatus incorporates several improvements over that used to prepare Na-NH_3 films,[7] the most significant being a change in which the molecular beam oven, except for its orifice, is shrouded with a liquid nitrogen jacket. This, along with the fact that the metallic constituent of the beam is Hg, which is extremely volatile, results in an energy flux less than 10^{-4} W/cm^2 at the substrate surface.

Film compositions quoted here are nominal in that they are determined from parameters of the oven. The composition of the beam was adjusted by regulating the pressure of Xe gas in the oven and by controlling the temperature of the oven so as to obtain the desired vapor pressure of Hg. The Hg and Xe were thus thoroughly mixed in the oven which served as the source for the molecular beam. Because the sticking coefficients of Hg and Xe are close to unity at the beam fluxes and substrate temperatures used here, the films should be random mixtures of the constituents with the composition of the vapor.[8] The conductances of films increased linearly with time at fixed deposition rates, indicating that the films are homogeneous in composition across their thicknesses. (A possible exception is in the first several atomic layers, for which the resistance was not measurable.) All electrical resistance measurements were made by use of a four-terminal technique in an ambient magnetic field of the order of 0.5 G. Measurements at temperatures above 10 K could not be made on as-prepared films as significant annealing was always observed above 10 K.

In Fig. 1 we plot, as functions of atomic concentration of Hg in mole percent metal (MPM), both the logarithm of the normal-state resistivity

